ACS APPLIED MATERIALS & INTERFACES

RESEARCH ARTICLE

www.acsami.org

A Universal Sensor for Mercury (Hg, Hg^{I}, Hg^{II}) Based on Silver Nanoparticle-Embedded Polymer Thin Film

G. V. Ramesh and T. P. Radhakrishnan*

School of Chemistry, University of Hyderabad, Hyderabad 500 046, India

Supporting Information

ABSTRACT: Detection of mercury at concentration levels down to parts-per-billion is a problem of fundamental and practical interest due to the high toxicity of the metal and its role in environmental pollution. The extensive research in this area has been focused primarily on specific sensing of mercuric (Hg^{2+}) ion. As mercury exists in the oxidation states, +2, +1 and 0 all of which are highly toxic, a universal sensor covering all the three while ensuring high sensitivity, selectivity, and linearity of response, and facilitating in situ as well as ex situ deployment, would be very valuable. Silver nanoparticle-embedded poly(vinyl alcohol) (Ag-PVA) thin film fabricated through a facile protocol is shown to be a fast, efficient and selective sensor for Hg^{2+}, Hg_2^{2+} and Hg in aqueous medium with a detection limit of 1 ppb. The sensor response is linear in the 10 ppb to 1 ppm concentration regime. A unique characteristic of the thin film based sensor is the blue shift occurring concomitantly with the decrease in the surface plasmon resonance absorption upon interaction with mercury, making the sensing highly selective. Unlike the majority of known sensors that work only in situ, the thin film sensor can be used ex situ as well. Examination of the thin film using microscopy and spectroscopy through the sensing process provides detailed insight into the sensing event.

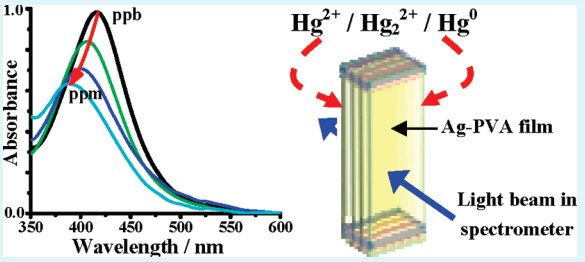

KEYWORDS: mercury, universal sensor, silver nanoparticle, polymer, thin film

INTRODUCTION

Mercury is highly toxic in all its oxidation states, 0, +1 and +2,[1−4] notwithstanding differences in solubilities and possible redox interconversions. As the maximum permissible level in food and drinking water is ∼2 ppb,[5] development of efficient sensors for mercury is of great interest. A variety of sensors based on electrochemical response and conductivity[6−8] as well as color and fluorescence[5,9−20] changes have been developed. Many operate only in nonaqueous solvents; direct sensing of elemental mercury has mostly been carried out in the vapor state.[21−23] Sensors that can be deployed in aqueous medium are of great practical utility. A wide range of mercury sensors based on metal nanoparticles have been developed in recent times.[24−38] Even though many are efficient and selective, the studies have targeted almost exclusively Hg^{2+} ions, exploiting specific complexation effects.[9−20,24−35] Tailored molecular structures including specialized DNA sequences and complex mechanisms are involved in many of the designs. A popular approach is to cap the nanoparticles with designer ligands and monitor the spectral shifts induced by nanoparticle aggregation triggered by the complexation of Hg^{2+} with the capping ligands.[24−29,35] Except for a few thin film sensors (which however do not exhibit very high sensitivity),[5,39−42] in most of the cases reported so far, the sensing agent is mixed with the analyte medium and the response recorded in situ. When optical responses like absorption or emission of the sensor are monitored, interference due to the analyte medium can render the sensor inefficient or ineffective. Packaging of these sensors is generally cumbersome and portability poor.

Silver forms amalgam with Hg and the redox potentials are appropriate for galvanic replacement reaction with Hg_2^{2+} and Hg^{2+}.[43] As adsorption of mercury ions, redox reaction with them, as well as amalgamation can sensitively influence the surface plasmon resonance (SPR) extinction of Ag nanoparticles, the latter provides a relatively cheap (compared to Au nanoparticle based sensors) and efficient (as the molar extinction coefficients are much higher than that of Au nanoparticles[35,44]) route to monitor mercury in all its oxidation states. Selectivity would be high as such reactions do not occur with the majority of transition metal ions. Ag nanoparticles in solution have been used for sensing Hg^{2+} based on the reduction of the SPR extinction; one of the studies showed slight blue shift of the peak during sensing,[37] whereas the other demonstrated clear red shifts due to aggregation.[38] The latter effect is observed with other analytes as well[45−47] and is expected to occur with ions like Au^{3+} which also oxidize Ag, compromising the selectivity of the sensing process. The higher sensitivity to oxidation and greater susceptibility to degradation during functionalization compared to Au, are some of the other handicaps of Ag nanoparticles.[35,48] We envisaged that embedding the Ag nanoparticles inside a polymer matrix would suppress degradation, and a sensing process based on

Received: September 16, 2010
Accepted: February 24, 2011
Published: March 11, 2011

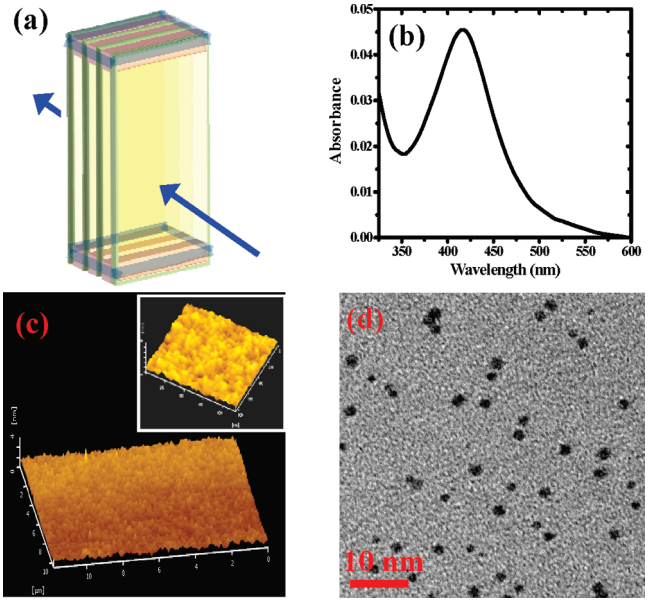

Figure 1. (a) Schematic diagram of the Ag-PVA thin film pack sensor; four film-coated glass plates (25 × 6 × 1.5 mm^3) packed with thin Teflon spacers at the two ends tied with Teflon tape form the sensor element; path of the light beam in the spectrometer is shown. (b) SPR spectrum, (c) AFM topography image (~ 12 μm × 10 μm × 4 nm); inset (~ 1 μm × 1 μm × 4 nm), and (d) TEM image (scale bar = 10 nm) of Ag-PVA thin film sensor.

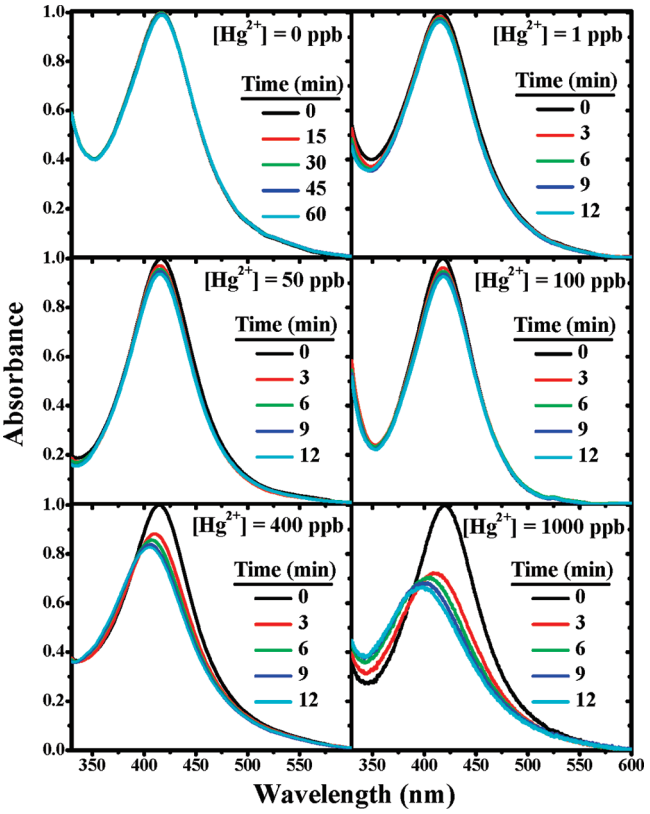

Figure 2. Temporal variation of the SPR spectra of Ag-PVA thin film immersed in aqueous solutions with different concentrations of Hg^{2+} (note the longer time interval for the case of pure water i.e., [Hg^{2+}] = 0 ppb); absorbance at λ_{max} at zero time is normalized to 1.0 in each case.

galvanic reaction/amalgamation would preclude the need for special functionalization of the nanoparticle. As the Hg formed by reduction of the ions is likely to remain as a shell around the Ag nanoparticle within the polymer matrix or form an amalgam, a blue shift of the SPR can be expected,[49−51] imparting remarkable selectivity for the sensing response. A polymer based thin film sensor that can be fabricated easily and cheaply, would not only be cost-effective, but also portable and easy to use. In addition to in situ sensing, it would allow ex situ analysis. The simple technique that we have optimized for the generation of silver[52−54] and other noble metal[55,56] nanoparticles inside poly(vinyl alcohol) (PVA) thin films is a convenient strategy to fabricate such a thin film sensor. The current study demonstrates the fast, efficient and selective sensing of mercury in the three oxidation states using Ag-PVA thin film showing detectable response down to the level of 1 ppb. Detailed investigations reveal a fast and highly linear response in the 10 ppb to 1 ppm range of mercury concentration. We illustrate also a unique advantage of the thin film based sensor, its amenability to detailed examination through the sensing event providing critical insight into the process involved.

RESULTS AND DISCUSSION

The nanocomposite thin film was fabricated using the protocol developed in our laboratory earlier (see Experimental Section for details)[52,53] with relevant changes in the polymer. Aqueous solutions of $AgNO_3$ and PVA were mixed in required proportions; PVA with a high average molecular weight (85 − 146 kDa) and hydrolysis (99+%) was used, so that following the heat treatment, the film is insoluble in the aqueous medium under the conditions used for sensing. The solution mixture was spin-coated on glass/quartz substrate. The film was subsequently heated, leading to the generation of Ag nanoparticles within the film matrix; the polymer functions as the reducing agent for Ag^+ as well as the stabilizer for the nanoparticles formed. The Ag/PVA weight ratio of 0.0075 and the fabrication condition of 130 °C for 2 h that resulted in an optimal concentration and size distribution of nanoparticles, and the design involving a pack of four thin films (Figure 1a) were arrived at on the basis of extensive experiments. The design ensured a sufficiently intense SPR spectrum with sensitivity to detect mercury from very low (ppb/nM) to high (ppm/μM) concentrations. The sensing response was found to be tolerant to small variations in the film fabrication conditions. The film was characterized by thickness measurement, electronic spectroscopy, atomic force microscopy (AFM), transmission electron microscopy (TEM) with energy-dispersive X-ray spectroscopy (EDXS), and X-ray photoelectron spectroscopy (XPS). Free-standing film fabricated using a sacrificial polystyrene layer[52−56] was used for direct TEM imaging; as the extremely thin film used for sensing was not amenable to this procedure, slightly thicker films with the same Ag/PVA composition was used. The Ag-PVA film on the substrate is ~50 nm thick,[43] facilitating easy access of the analyte to the Ag nanoparticles. Figure 1b shows the SPR spectrum with λ_{max} at 418 nm typical of Ag nanoparticles; there is very little scattering and the spectrum is primarily due to absorption. The smooth (average roughness ~0.30 nm) surface morphology is revealed by the AFM image (Figure 1c). The TEM image (Figure 1d) shows Ag nanoparticles with diameters ~1 − 2 nm.

The SPR spectrum of the sensor film pack immersed in pure water remains constant for >1 h (Figure 2), demonstrating that

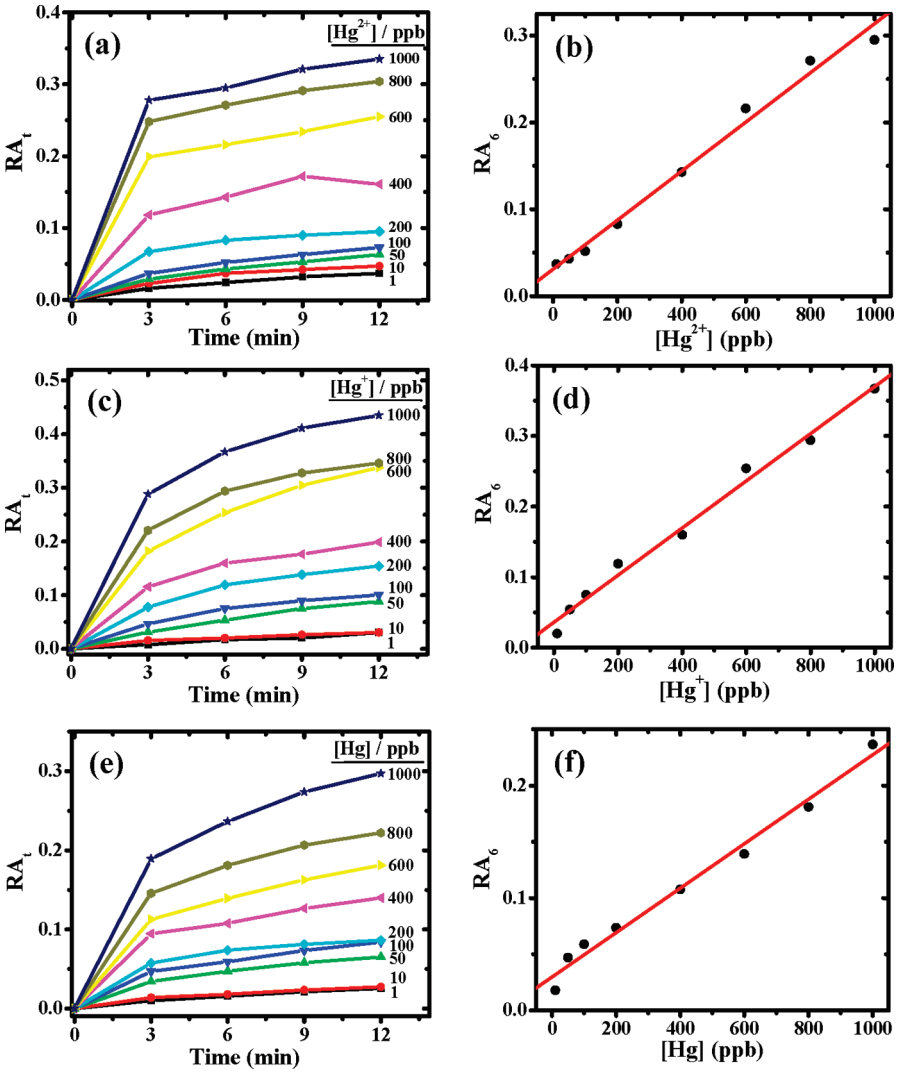

Figure 3. Relative change in absorbance, RA_t as a function of time for different concentrations of the analyte in aqueous medium (with trace PVA as stabilizer in the case of Hg), (a) Hg^{2+}, (c) Hg_2^{2+} ($[Hg^+] = 1/2[Hg_2^{2+}]$), and (e) Hg. Variation of RA_6 with the analyte concentrations (10 ppb −1 ppm): (b) $[Hg^{2+}]$, (d) $[Hg^+]$, and (f) [Hg]; the least-squares fit to a straight line is indicated in each case.

even though the polymer swells in the aqueous medium, there is absolutely no leaching of Ag. This was confirmed further by the observation of an identical spectrum for the same film pack removed from the water and dried. We describe first, the sensing experiments with aqueous solutions of Hg^{2+} (see Experimental Section for details). SPR spectra of the sensor film were recorded on introducing $Hg(NO_3)_2$ solution. The spectra for a selected set of concentrations are shown in Figure 2; the complete set is provided in the Supporting Information. The spectra show small but definite and reproducible decrease in intensity within a few minutes, even at the lowest concentration of 1 ppb. With concentrations close to 1 ppm, the spectrum shows significant change even within 3 min. In addition to the decrease in intensity, the peak undergoes a blue shift which becomes prominent at higher concentrations. The relative change in absorbance, RA_t at time t can be defined as $[\{A_{max}(0) - A_{max}(t)\}/A_{max}(0)]$, where $A_{max}(t)$ is the absorbance at the λ_{max} of the spectrum at time t. Plot of RA_t versus t, for different concentrations of Hg^{2+} are shown in Figure 3a; the errors in the values are typically <1.0%. There is little variation in the RA_t values below 10 ppb as the absolute values themselves are quite small. However, the RA_t values show excellent linear correlation with the concentration of Hg^{2+} over the wide range, 10 ppb to 1 ppm at $t \leq 12$ min;[43] the correlation is poorer at longer time scales. The response being linear at short time scales is indeed advantageous; Figure 3b illustrates the case of RA_6 with a correlation coefficient >0.99. Decrease in the absorbance can be attributed to the oxidation of Ag atoms in the nanoparticles by Hg^{2+}. The blue shift of the SPR peak most likely arises because of the formation of a shell of mercury with or without amalgamation on the surface of the nanoparticles, and the impact of the mercury shell on the plasmon resonance. Similar blue shifts of the SPR spectra have been reported in earlier studies on the interaction of Hg with colloidal Ag and Au.[49−51] Calculations based on a core−shell model were consistent with the observed blue shift of the SPR absorption peak.[51]

Similar spectral responses are elicited by aqueous solutions containing mercurous ions (Hg_2^{2+} in solution was independently confirmed by standard tests; see Experimental Section). As in the case of Hg^{2+}, a clear blue shift of the peak is observed at higher concentrations of Hg_2^{2+}. Again RA_t increases with

concentration and time (Figure 3c); the linear correlation of RA_6 with the concentration of Hg_2^{2+} ($r > 0.99$) is shown in Figure 3d. We have also explored the utility of the Ag-PVA film in the detection of elemental mercury. The solubility of mercury in water at 298 K is 63.9 μg/l (~64 ppb);[57,58] higher concentrations may be stabilized by the presence of organics, possibly facilitating its mobility in the environment. We prepared aqueous solutions containing mercury up to ppm levels; trace amounts of PVA was added to prevent coalescence (see Experimental Section). The resulting solution is transparent and stable; the absolute concentration of Hg was determined by ICP-OES analysis and the solution diluted appropriately to prepare lower concentrations of Hg. SPR spectra of the Ag-PVA film immersed in these solutions showed trends similar to that in the previous cases;[43] plots of RA_t are shown in Figure 3e and the linear correlation of RA_6 with the concentration of Hg ($r > 0.99$) in Figure 3f. As Ag is not oxidized in this case, the spectral changes can be attributed to amalgamation at the surface of the nanoparticles involving partial dissolution of the nanoparticles.

It is important to consider the binding forces that lead to the interaction of mercury atoms/ions with the Ag-PVA sensor film. PVA is known to bind to metal ions through the oxygen atoms; in fact such coordinative interactions have been implicated as the first step in the process of Ag^+ reduction by PVA.[59] It is likely that the mercury ions also bind the same way. Swelling of the PVA film in the aqueous medium facilitates the diffusion of mercury atoms/ions into the polymer matrix. The galvanic reaction and/or amalgamation with the Ag nanoparticles cause the concentration of the mercury atoms/ions in the vicinity of the nanoparticles to drop, triggering diffusion from the bulk solution. Because the sensor action is based on a chemical process, we have explored the temperature dependence of the sensor response by carrying out experiments for the typical case of $[Hg^{2+}]$ = 200 ppb in the range 20−80 °C. As expected, the response is found to increase with temperature.[43] The dependence of RA_t on temperature is nearly linear for each of the time points suggesting that the sensor would function effectively in this temperature range.

The thin film nature of the sensor facilitates convenient monitoring of the sensor through the sensing process. AFM images show that the film is intact throughout, the mean roughness remaining nearly the same (~0.29 nm).[43] TEM images (Figure 4a−c) reveal a clear decrease in the density of nanoparticles upon immersion in aqueous solutions of Hg^{2+} ions or Hg; significantly, those that remain appear larger. A careful examination of the temporal evolution of the images under the electron beam reveals interesting features. The particles in the Ag-PVA films dipped in pure water and solution of Hg are quite stable.[43] However, in the case of the film dipped in Hg^{2+} solution, a lower-magnification image (Figure 4d) showed some large structures disappearing within ~60 s with a characteristic meniscus formed in between, whereas the relatively smaller ones remained intact. These observations suggest that, the reduction of Hg^{2+} by small Ag nanoparticles leads to the complete oxidation of Ag (which goes into solution) and formation of pure Hg droplets inside the polymer film which possibly coalesce into larger drops; these tend to evaporate under the electron beam. In the case of slightly larger Ag nanoparticles, the Hg formed by reduction generates an amalgam, which is stable under the beam. These inferences are validated by the EDX spectra[43] recorded on the large particle region showing the presence of mercury alone and those recorded on the small particle region showing the presence of both

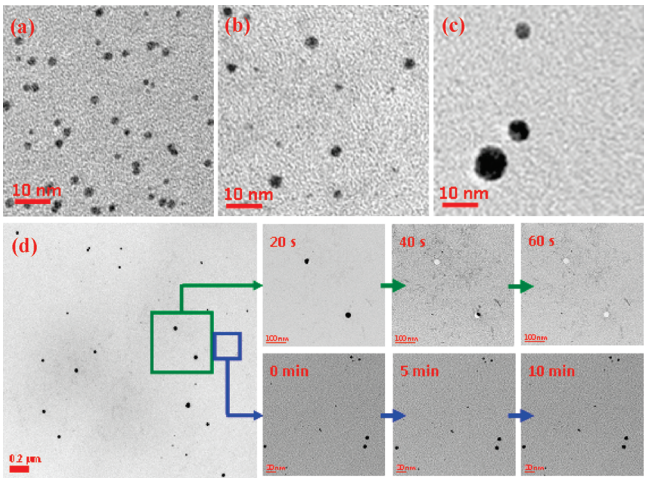

Figure 4. TEM images of Ag-PVA film immersed for 12 min in (a) pure water, (b) an aqueous solution of 1 ppm Hg^{2+} ions and (c) an aqueous solution of 1 ppm Hg (with trace PVA); scale bar =10 nm. (d) Temporal evolution of different nanostructures in the film immersed in the Hg^{2+} solution, under the electron beam; two selected regions in a larger area image are shown for different time periods and with different magnifications in order to highlight the observations; top panel: 20−60 s, scale bar = 100 nm; bottom panel: 0−10 min, scale bar = 20 nm).

silver and mercury. In the case of Ag-PVA dipped in the solution of Hg, there is only amalgam formation, and hence all the particles are stable under the electron beam; presence of mercury and silver is confirmed by the EDX spectrum. Both the Hg droplets and the Ag amalgam possibly have higher mobility inside the PVA film, leading to limited aggregation and increase in particle size. EDX spectra of Ag-PVA film show the presence of Ag alone and no Hg as expected. XPS data collected on the various films provide further support for the conclusions drawn above.[43]

As noted above, the characteristic response of earlier Ag nanoparticle based sensors has largely involved red shift of the SPR spectra.[38,45−47] The definitive blue shift in the present case of mercury sensing imparts remarkable selectivity. This aspect can be exploited by including the peak shift, $\Delta\lambda_t = [\lambda_{max}(0) - \lambda_{max}(t)]$ in the sensor response. The value $\Delta\lambda_6$*RA_6 for different analytes plotted in Figure 5 illustrates the high selectivity of the present universal mercury sensor. As expected based on the reduction potentials, the Ag-PVA film is insensitive to most of the metal ions.[43] Typical examples like K^+, Mn^{2+}, Fe^{2+}, Ni^{2+}, Zn^{2+}, Cd^{2+}, Cu^{2+}, Ag^+, and Pb^{2+}, even at 10 ppm concentrations, show far weaker responses than mercury at a few hundred ppb levels. An oxidizing acid like HNO_3 also elicits little response up to high concentrations like 10 ppm. Redox potentials indicate that Au^{3+} can oxidize Ag. The SPR absorption is indeed diminished by $HAuCl_4$; however, the peak shows a clear red shift,[43] as the effect is quite distinct from that of mercury. The contrasting observation with respect to Ag nanoparticle solution based sensors[37,38] signifies the superiority of the nanocomposite thin film sensor. The control experiments prove that, even though some analytes affect the SPR response of the Ag-PVA film sensor, mercury is easily distinguished by the characteristic and conspicuous blue shift it induces. We have examined also the capability of Ag-PVA thin film for ex situ monitoring of mercury. Films were immersed for different time periods in an aqueous solution of Hg_2^{2+}, taken out, washed in water and dried. The

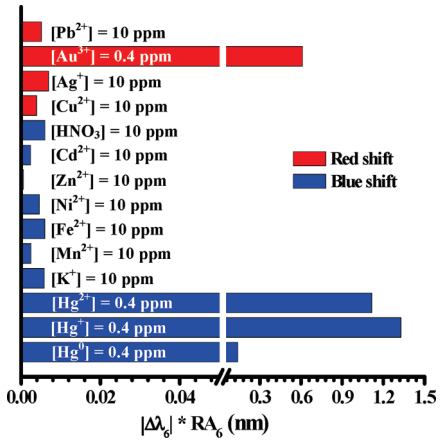

Figure 5. Comparison of the response of the Ag-PVA film sensor, $|\Delta\lambda_6|$*RA_6 (see text for definition) to different analytes; the concentration level of the aqueous solutions are indicated in terms of the metal ion or the molecule in the case of HNO_3.

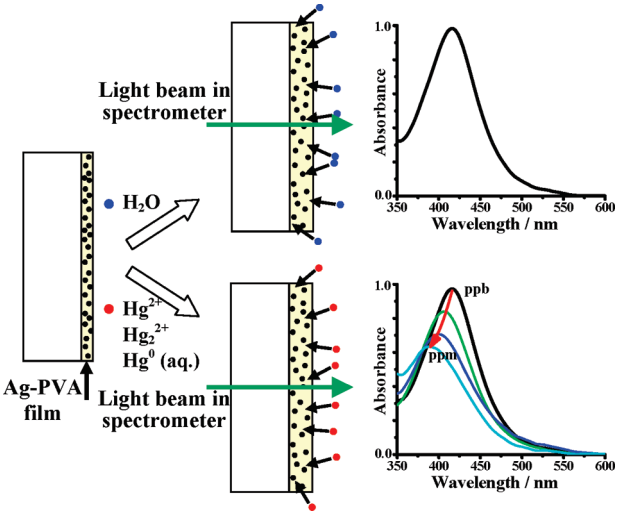

Figure 6. Schematic representation of the swelling of the Ag-PVA film in aqueous medium and the sensitive changes in the SPR spectrum of the film induced by $Hg^{2+}/Hg_2^{2+}/Hg^0$ in the solution.

SPR spectra showed responses very similar to that in the in situ studies,[43] establishing the feasibility of packaging, and the portability of the thin film sensor.

A combination of the observed SPR spectral responses of Ag-PVA film exposed to the various analytes, temporal evolution of the spectra, and the microscopy characterization of the sensor films through the sensing process discussed above provide significant insight into the sensing process and the underlying mechanism. The overall process is represented schematically in Figure 6. The film immersed in pure water exhibits the SPR spectrum due to the embedded Ag nanoparticles. Exposure to mercury atoms or ions present in the aqueous medium cause clear decay and blue shift in the SPR extinction profile. Although most other metal ions elicit negligible response, gold ions induce decay with a red shift. These observations clearly prove that ions capable of oxidizing silver as well as elemental mercury that forms an amalgam cause decay of the SPR absorption of the silver nanoparticles. Most significantly, the presence of mercury on the silver nanoparticles embedded within the polymer film leads to a blue-shifted peak. The microscopy characterizations of the films after the sensing process provide evidence for the presence of mercury in the films. The initial kinetics of the process is controlled by the diffusion of mercury atoms or ions to the silver nanoparticles inside the swollen polymer film. This is likely to be an important factor that gives rise to the linear variation of the spectral responses with the analyte concentration observed at short time scales. The linearity does not hold at longer time scales, possibly because of the enveloping of the silver nanoparticles with the mercury and the impact of this on the kinetics of further sensor-analyte interaction.

CONCLUSIONS

The present study illustrates the design of a simple, nanocomposite thin film sensor based on silver nanoparticles embedded in poly(vinyl alcohol) fabricated through a facile in situ fabrication protocol. Fast, sensitive and selective detection of mercury in all its oxidation states is demonstrated in this study; the thin film matrix facilitates the observation of the characteristic blue shift of the SPR spectrum upon interaction with mercury, enhancing the selectivity of the detection. Low-cost, linear response over a wide range of concentrations, ease of deployment and the feasibility of both in situ and ex situ analysis are prominent features of the thin film sensor. The sensor can be either integrated with a portable fiber-optic spectrometer for on-site detection or packaged into strips for ex situ detection and quantitative estimation of mercury. The present study demonstrates the unique potential of metal nanoparticle-embedded polymer thin films in chemical sensing applications. The scope for further development of this concept is extensive, in view of the flexibility and versatility of these nanocomposite materials.

EXPERIMENTAL SECTION

Fabrication of Ag-PVA Film. One and a half milligrams of $AgNO_3$ was dissolved in 0.75 mL of water, and mixed with 2.53 mL of a solution of poly(vinyl alcohol) (PVA; Aldrich, average molecular weight = 85−146 kDa, % hydrolysis = 99+) in water (1 g PVA dissolved in 20 mL of water with mild heating); the resulting weight ratio of Ag/PVA is 0.0075. The solution mixture was diluted by adding 2.72 mL of water and stirred for 10 min at the ambient temperature of 25 °C. The solution was always protected from light. Milli-Q purified water was used in all operations. Glass substrates were cleaned in soap solution and water followed by sonication with isopropyl alcohol for 10 min and dried in a hot air oven. The $AgNO_3$−PVA solution was spin-coated on the glass substrate using a Laurell Technologies Corporation Model WS-400B-6NPP/LITE/8K Photoresist Spinner operated at 500 rpm for 10 s followed by 8000 rpm for 10 s. The film was heated in a hot air oven at 130 °C for 2 h. To prepare thicker films for TEM samples, the initial solution mixture (excluding the dilution with 2.72 mL of water) was used. The substrate was prepared by first spin-coating a few drops of a solution of 1 g of polystyrene (PS, average molecular weight = 280 kDa) in 8 mL of toluene at 1,000 rpm for 10 s, followed by drying in a hot air oven at 85−90 °C for 20 min. The $AgNO_3$−PVA solution was coated on top of the PS layer by spinning at 500 rpm for 10 s followed by 8000 rpm for 10 s and subsequently heated at 90 °C for 3 h. The film was then cut and peeled off the glass and placed on a 200 mesh TEM copper grid and dipped in toluene, whereupon PS alone dissolved out.

Characterization of Ag-PVA Film. The Ag/PVA film was imaged using FEI TECNAI G^2 S-Twin transmission electron microscope at an accelerating voltage of 200 kV; the time for recording an image was ∼6 s

(1335 × 1344 pixels; 2 s exposure). EDX spectra were recorded on FEI TECNAI G^2 TEM equipped with a GIF camera. XPS analysis was carried out on a KESCA+Omicron Spectrometer with a monochromatic Al K_α X-ray source (1486.6 eV); the X-ray power supply was run at 15 kV and 5 mA and the pressure in the analysis chamber during the scans was 1×10^{-9} Torr. Electronic spectra were recorded on a Cary 100 Bio or a Perkin-Elmer Lambda 35 UV−visible Spectrophotometer. AFM images were recorded using a SEIKO model SPA 400 atomic force microscope in the dynamic force mode using a cantilever with a force constant of 12 N/m; roughness was analyzed using the software provided by the manufacturer. Thickness of the films was measured using an Ambios Technology XP-1 profilometer.

Preparation of Analyte Solutions. Millipore Milli-Q water (resistivity = 18 MΩ cm) was used in all preparations. Mercury(II) nitrate (Aldrich, volumetric standard, 0.14 N solution in water) was diluted appropriately with water to prepare the analyte solutions with concentrations ranging from 1 ppb to 1 ppm of Hg^{2+}; the highest concentration was independently confirmed by inductively coupled plasma-optical emission spectrometer (ICP-OES, Varian Model Liberty Series). Ten milligram of mercurous nitrate (Merck, 97%) was dissolved in 0.2 mL of ∼0.3 N nitric acid and diluted appropriately with water to prepare the analyte solutions with concentrations ranging from 1 ppb to 1 ppm of Hg_2^{2+}; the highest concentration was independently confirmed by ICP-OES analysis. As Hg_2^{2+} can disproportionate into Hg^{2+} and Hg^0, we have carried out a standard test to confirm the presence of Hg_2^{2+} in the solutions prepared.[60] The characteristic test for Hg_2^{2+} involved addition of excess thiocyanate and ferric ion and the detection of the ferrous ions (formed by the reduction of ferric by mercurous ions) using *o*-phenanthroline (after masking the ferric thiocyanate with fluoride); a characteristic red precipitate extractable in amyl alcohol confirmed the presence of Hg_2^{2+}. It may be noted that other ions including Hg^{2+} do not give this positive test. Hg solutions were prepared as follows. One gram of PVA (Aldrich, average molecular weight = 85−146 kDa, % hydrolysis = 99+), was dissolved in 20 mL of warm water. Two and a half grams of mercury (Merck Pure) was added to 50 mL of water taken in a round-bottom flask and sonicated for 5 min. Three-tenths of a milliliter of this mixture was transferred immediately to 80 mL water containing 1 mL of the PVA solution prepared above. This final solution was found to be transparent and stable. Typical concentration of mercury obtained in the solution was ∼1 ppm; the exact concentration was determined using ICP-OES analysis and this solution was diluted appropriately with water to prepare analyte solutions having concentrations ranging from 1 ppb to 1 ppm of Hg.

Sensing Experiments. All experiments (except those related to the temperature dependence) were carried out at the ambient temperature of 25 °C. The sensor film pack (Figure 1a) was immersed in ultrapure water (Millipore Milli-Q, resistivity = 18 MΩ cm) taken in a spectrometer cuvette, for 20 min; the SPR spectrum of the film was monitored during this time. The water was removed completely and replaced with the analyte solution. The SPR spectrum of the film was monitored for up to 20 min. A fresh film pack was used for each new experiment. The reproducibility of the sensing process was examined by running repeated batches of selected experiments.[43] The standard deviations in the RA_t values for different time points were found to be typically ∼0.7−0.8%. indicating a high level of reproducibility.

■ ASSOCIATED CONTENT

Supporting Information. Details of sensing experiments, sensor monitoring, and control studies (PDF). This material is available free of charge via the Internet at http://pubs.acs.org/.

■ AUTHOR INFORMATION

Corresponding Author

*E-mail: tprsc@uohyd.ernet.in. Fax: 91-40-2301-2460. Phone: 91-40-2313-4827.

■ ACKNOWLEDGMENT

Financial support from the DST, New Delhi, infrastructure support from the Centre for Nanotechnology at the University of Hyderabad and a senior research fellowship for GVR from CSIR, New Delhi are gratefully acknowledged. We thank Mr. M. Durga Prasad and Mr. E. Manohar Reddy for help with the TEM imaging. We thank also the International Advanced Research Centre for Powder Metallurgy and New Materials, Hyderabad, and Dr. N. Hebalkar for providing the EDXS and XPS data.

■ REFERENCES

(1) Clarkson, T. W. *Crit. Rev. Clin. Lab. Sci.* **1997**, *34*, 369.
(2) Goldman, L. R.; Shannon, M. W. *Pediatrics* **2001**, *108*, 197.
(3) Berlin, M.; Zalups, R. K.; Fowler, B. A. In *Handbook on the Toxicology of Metals*, 3rd ed.; Nordberg, G. F., Fowler, B. A., Nordberg, M., Friberg, L. T.), Eds.; Elsevier: New York, 2007; p 675.
(4) Holmes, P.; James, K. A. F.; Levy, L. S. *Sci. Total Environ.* **2009**, *408*, 171.
(5) Nolan, E. M.; Lippard, S. *Chem. Rev.* **2008**, *108*, 3443.
(6) Wang, J.; Tian, B.; Lu, J.; Wang., J.; Luo, D.; MacDonald, D. *Electroanalysis* **1998**, *10*, 399.
(7) Mor-Piperberg, G.; Tel-Vered, R.; Elbaz, J.; Willner, I. *J. Am. Chem. Soc.* **2010**, *132*, 6878.
(8) Lee, M.; Lee, J.; Kim, T. H.; Lee, H.; Lee, B. Y.; Park, J.; Jhon, Y. M.; Seong, M.; Hong, S. *Nanotechnology* **2010**, *21*, 055504.
(9) Ono, A.; Togashi, H. *Angew. Chem., Int. Ed.* **2004**, *43*, 4300.
(10) Zhu, X.; Fu, S.; Wong, W.; Guo, J.; Wong., W. *Angew. Chem., Int. Ed.* **2006**, *45*, 3150.
(11) Kim, I.; Bunz, U. H. F. *J. Am. Chem. Soc.* **2006**, *128*, 2818.
(12) Zhao, Y.; Zhong, Z. *J. Am. Chem. Soc.* **2006**, *128*, 9988.
(13) Liu, J.; Lu, Y. *Angew. Chem., Int. Ed.* **2007**, *46*, 7587.
(14) Wegner, S. V.; Okesli, A.; Chen, P.; He, S. *J. Am. Chem. Soc.* **2007**, *129*, 3474.
(15) Chiang, C.; Huang, C.; Liu, C.; Chang, H. *Anal. Chem.* **2008**, *80*, 3716.
(16) Loe-Mie, F.; Merchand, G.; Berthier., J.; Sarrut, N.; Pucheault, M.; Blanchard-Desce, M.; Vinet, F.; Vaultier, M. *Angew. Chem., Int. Ed.* **2010**, *49*, 424.
(17) Lin, W.; Cao, X.; Ding, Y.; Yuan, L.; Long, L. *Chem. Commun.* **2010**, *46*, 3529.
(18) Dave, N.; Chan, M. Y.; Huang, P. J.; Smith, B. D.; Liu, J. *Am. Chem. Soc.* **2010**, *132*, 12668.
(19) Shi, H.; Liu, S.; Sun, H.; Xu, W.; An, Z.; Chen, J.; Sun, S.; Lu, X.; Zhao, Q.; Huang, W. *Chem.—Eur. J.* **2010**, *16*, 12158.
(20) Dong, M.; Wang, Y.; Peng, Y. *Org. Lett.* **2010**, *12*, 5310.
(21) McNerney, J. J.; Buseck, P. R.; Hanson, R. C. *Science* **1972**, *178*, 611.
(22) Rogers, B.; Manning, L.; Jones, M.; Sulchek, T.; Murray, K.; Beneschott, B.; Hu, Z.; Thundat, T.; Cavazos, H.; Minne, S. C. *Rev. Sci. Instrum.* **2003**, *74*, 4899.
(23) Drelich, J.; White, C. L.; Xu, Z. *Environ. Sci. Technol.* **2008**, *42*, 2072.
(24) Huang, C.; Chang, H. *Chem. Commun.* **2007**, 1215.
(25) Lee, J.; Han, M. S.; Mirkin, C. A. *Angew. Chem., Int. Ed.* **2007**, *46*, 4093.
(26) Huang, C.; Yang, Z.; Lee, K.; Chang, H. *Angew. Chem., Int. Ed.* **2007**, *46*, 6824.
(27) Li, D.; Wieckowska, A.; Willner, I. *Angew. Chem., Int. Ed.* **2008**, *47*, 3927.

(28) Xue, X.; Wang., F.; Liu, S. *J. Am. Chem. Soc.* **2008**, *130*, 3244.
(29) Kim, Y.; Mahajan, R. K.; Kim, J. S.; Kim, H. *ACS Appl. Mater. Interfaces* **2010**, *2*, 292.
(30) Xie, J.; Zheng, Y.; Ying, J. Y. *Chem. Commun.* **2010**, *46*, 961.
(31) Darbha, G. K.; Ray, A.; Ray, P. C. *ACS Nano* **2010**, *1*, 208.
(32) Darbha, G. K.; Singh, A. K.; Rai, U. S.; Yu, E.; Yu, H.; Ray, P. C. *J. Am. Chem. Soc.* **2008**, *130*, 8038.
(33) Adhikari, B.; Banerjee, A. *Chem. Mater.* **2010**, *22*, 4364.
(34) Bera, R. K.; Das, A. K.; Raj, C. R. *Chem. Mater.* **2010**, *22*, 4505.
(35) Wang, Y.; Yang, F.; Yang, X. *ACS Appl. Mater. Interfaces* **2010**, *2*, 339.
(36) Rex, M.; Hernandez, F. E.; Campiglia, A. D. *Anal. Chem.* **2006**, *78*, 445.
(37) Fan, Y.; Liu, Z.; Wang, L.; Zhan., J. *Nanoscale Res. Lett.* **2009**, *4*, 1230.
(38) Li, W.; Guo, Y.; McGill, K.; Zhang, P. *New J. Chem.* **2010**, *34*, 1148.
(39) Palomares, E.; Vilar, R.; Durrant, J. R. *Chem. Commun.* **2004**, 362.
(40) Coronado, E.; Galán-Mascarós, J. R.; Martí-Gastaldo, C.; Palomares, E.; Durrant, J. R.; Vilar, R.; Gratzel, M.; Nazeeruddin, M. K. *J. Am. Chem. Soc.* **2005**, *127*, 12351.
(41) Cheng, X.; Li, Q.; Qin, J.; Li, Z. A. *ACS Appl. Mater. Interfaces* **2010**, *2*, 1066.
(42) Liu, N.; Li, L.; Caob, G.; Lee, R. *J. Mater. Chem.* **2010**, *20*, 9029.
(43) See the Supporting Information.
(44) Thompson, D. G.; Stokes, R. J.; Martin, R. W.; Lundahl, R. J.; Faulds, K.; Graham, D. S. *Small* **2008**, *4*, 1054.
(45) Dubas, S. T.; Pimpan, V. *Mater. Lett.* **2008**, *62*, 3361.
(46) Gradess, R.; Abargues, R.; Habbou, A.; Canet-Ferrer, J.; Pedrueza, E.; Russell, A.; Valdés, J. L.; Martínez-Pastor, J. P. *J. Mater. Chem.* **2009**, *19*, 9233.
(47) Li, H.; Yao, Y.; Han, C.; Zhan, J. *Chem. Commun.* **2009**, 4812.
(48) Wei, H.; Chen, C.; Han, B.; Wang, E. *Anal. Chem.* **2008**, *80*, 7051.
(49) Katsikas, L.; Guttiérrez, M.; Henglein, A. *J. Phys. Chem.* **1996**, *100*, 11203.
(50) Henglein, A.; Brancewicz, C. *Chem. Mater.* **1997**, *9*, 2164.
(51) Morris, T.; Copeland, H.; McLinden, E.; Wilson, S.; Szulczewski, G. *Langmuir* **2002**, *18*, 7261.
(52) Porel, S.; Singh, S.; Harsha, S. S.; Rao, D. N.; Radhakrishnan, T. P. *Chem. Mater.* **2005**, *17*, 9.
(53) Ramesh, G. V.; Porel, S.; Radhakrishnan, T. P. *Chem. Soc. Rev.* **2009**, *38*, 2646.
(54) Ramesh, G. V.; Sreedhar, B.; Radhakrishnan, T. P. *Phys. Chem. Chem. Phys.* **2009**, *11*, 10059.
(55) Porel, S.; Singh, S.; Radhakrishnan, T. P. *Chem. Commun.* **2005**, 2387.
(56) Porel, S.; Hebalkar, N.; Sreedhar, B.; Radhakrishnan, T. P. *Adv. Funct. Mater.* **2007**, *17*, 2550.
(57) Sanemasa, I. *Bull. Chem. Soc. Jpn.* **1975**, *48*, 1795.
(58) Clever, H. L.; Johnson, S. A.; Derrick, M. E. *J. Phy. Chem. Ref. Data* **1985**, *14*, 631.
(59) Clémenson, S.; David, L.; Espuche, E. *J. Polym. Sci., A: Polym. Chem.* **2007**, *45*, 2657.
(60) Lucena-Conde, F. *Microchim. Acta* **1952**, *40*, 8.